Regularized Constrained Total Least Squares Image Restoration

Vladimir Z. Mesarović, Nikolas P. Galatsanos, *Member, IEEE,*
and Aggelos K. Katsaggelos, *Senior Member, IEEE*

Abstract— **In this paper, the problem of restoring an image distorted by a linear space-invariant (LSI) point-spread function (PSF) that is not exactly known is formulated as the solution of a perturbed set of linear equations. The regularized constrained total least-squares (RCTLS) method is used to solve this set of equations. Using the diagonalization properties of the discrete Fourier transform (DFT) for circulant matrices, the RCTLS estimate is computed in the DFT domain. This significantly reduces the computational cost of this approach and makes its implementation possible even for large images. An error analysis of the RCTLS estimate, based on the mean-squared-error (MSE) criterion, is performed to verify its superiority over the constrained total least-squares (CTLS) estimate. Numerical experiments for different errors in the PSF are performed to test the RCTLS estimator. Objective and visual comparisons are presented with the linear minimum mean-squared-error (LMMSE) and the regularized least-squares (RLS) estimator. Our experiments show that the RCTLS estimator reduces significantly ringing artifacts around edges as compared to the two other approaches.**

I. Introduction

THE restoration of degraded images is an important problem because it allows the recovery of lost information from the observed degraded image data [2]. Two kinds of degradations are usually encountered: spatial degradations (e.g., the loss of resolution) caused by blurring and point degradations (e.g., additive random noise), which affect only the gray levels of the individual picture points. Common types of spatial blurring are due to atmospheric turbulence, lens aberrations, and motion. Common types of point degradations are photochemical, photoelectronic, and electronic random noise. Spatial degradations, due to their lowpass nature, are ill-conditioned, therefore difficult to invert in the presence of noise [2], [4]. The purpose of image restoration is to produce the best estimate of the source image, given the recorded data and some *a priori* knowledge. Regularization is a general and very effective approach in ill-posed recovery problems [4]. According to this approach, to obtain the "best" solution, recorded data and *a priori* knowledge are used in a complementary way. The smoothness properties of the image are captured by the regularization operator while the regularization parameter trades off fidelity to the available data to smoothness of the solution [20], [6].

Traditionally, the point-spread function (PSF) of a spatially degrading system is assumed to be known [2]. Realistically speaking, however, the analyst is often faced with imprecise knowledge of the PSF. For example, such instances could occur in medical imaging, astronomy, and photography. In these cases, there are various reasons that do not allow the precise knowledge of the PSF. For example, in astronomy, atmospheric turbulence yields a time-varying PSF; in photography the camera with which a picture was taken may not be available. In those cases two approaches have been taken. With the first approach, restoration and simultaneous identification of the unknown/partially known PSF is attempted, see, for example [12], [13], [18], [23], or the PSF estimation from noisy measured data taken from a known point-source is performed prior to restoration [19]. The latter is the common practice in the astronomical community and it may be the source of errors in the PSF. With the second approach, a random variation is used to model the uncertainties in the PSF and this random model is incorporated in the restoration algorithm. In other words, with the second approach, more precise estimation of the PSF is not attempted, see for example [3], [5], [9], [21], [22].

In [21], [22], and [9], the PSF was assumed to contain a known deterministic mean and an additive random component with known statistics. A linear minimum mean-squared-error filters (LMMSE) were developed that explicitly incorporated the random component of the PSF. In [3], a similar problem was solved using the theory of projections onto convex sets [24].

Fan, in [5], addressed for the first time the problem of restoring 1-D signals from noisy measurements of *both* the PSF and the observed data as a regularized constrained total least-squares (RCTLS) problem. The data formation equation for this problem is the noise perturbed set of linear equations, $\mathbf{H}\,\mathbf{f} = \mathbf{g}$, where the matrix $\mathbf{H}$ models the blurring system and $\mathbf{g}$ and $\mathbf{f}$ are the observed and source data, respectively. It is well known that total least-squares (TLS) is a technique for solving this set of noise contaminated equations [7], [10]. The constrained total least-squares (CTLS) technique handles effectively the case when the noise elements in both $\mathbf{H}$ and $\mathbf{g}$ are linearly related and have equal variances [1]. In [5], it

Manuscript received February 1, 1994; revised October 14, 1994. This work was supported by the NSF grant MIP-9309910. The associate editor coordinating the review of this paper and approving it for publication was Dr. Reginald L. Lagendijk.

V. Mesarović and N. Galatsanos are with the Department of Electrical and Computer Engineering, Illinois Institute of Technology, Chicago, Illinois 60616 USA.

A. Katsaggelos is with the Department of Electrical Engineering and Computer Science, Northwestern University, Evanston, Illinois 60208 USA.

IEEE Log Number 9412462.

was assumed that *both* $\mathbf{H}$ and $\mathbf{g}$ are subject to the *same* errors that are modeled as additive noise. Accordingly, the proposed restoration scheme in [5] is based on a modified version of the CTLS approach as presented in [1]. The modification proposed in [5] was the addition of a regularization term to the function used for the CTLS formulation in [1]. The minimization of this function resulted in the RCTLS estimator. In addition, a perturbation analysis was performed and the bias and the variance of the RCTLS and the CTLS estimators were compared. However, the mean-squared-error (MSE) of the two estimators was not compared.

In this paper, the problem of restoring an image degraded by additive noise and a linear space-invariant (LSI) system that is not known exactly is examined. The image formation equation for this problem is similar to the one used in [5]. However, we assume that $\mathbf{H}$ and $\mathbf{g}$ are subject to *different* errors that are modeled as additive noises with different statistical properties. Accordingly, the proposed restoration scheme is based on a modified version of the RCTLS approach as presented in [5]. Since the main focus of this work is the restoration of images, the computational cost of the proposed filter is a major consideration. The RCTLS estimate in [5] is hard to compute for large 1-D signals, let alone images. Therefore, in this paper the circulant approximation for the PSF and the diagonalization properties of the discrete Fourier transform (DFT) are used. The benefits of this approximation are threefold: first, in the DFT domain, the computations required by the RCTLS filter are decoupled into a set of much simpler ones, and thus the implementation of the RCTLS filter is very efficient even for very large images. Second, unlike [5], where only the identity operator can be used for regularization operator, a general operator is used in our formulation. Based on the correspondence between constrained least-squares and maximum *a posteriori* (MAP) estimation (see for example [6]), the use of the identity operator implies that the underlying signal is white. For most signals of interest this is an unrealistic approximation that yields suboptimal results. Finally, using the DFT domain, a more conclusive study of the RCTLS and CTLS estimators than in [5] is performed. The MSE's of the two estimators are compared and we show that the MSE of the RCTLS estimator is smaller than its CTLS counterpart. Furthermore, the bounds for the regularization parameters that minimize the MSE of the RCTLS estimate are found. In addition, we show that the MSE analysis of the regularized least-squares (RLS) estimator in [6] can be obtained as a special case of the MSE analysis of the RCTLS estimator.

The rest of the paper is organized as follows. In Section II, the image restoration problem with an incorrectly known PSF is formulated as a CTLS problem. In Section III, we present the RCTLS approach and propose the unconstrained minimization of the RCTLS functional in the DFT domain. The error analysis is performed in Section IV, where we examine the MSE behavior of the RCTLS estimator for small noise levels. In Section V, experimental comparisons with the LMMSE and the RLS estimators for different types of PSF errors are provided. Finally, in Section VI we present our conclusions and suggestions for future research.

II. Constrained Total Least Squares Image Restoration

We assume that the $N \times 1$ PSF can be represented by

$$\mathbf{h} = \bar{\mathbf{h}} + \Delta\mathbf{h} \tag{1}$$

where $\bar{\mathbf{h}}$ and $\Delta\mathbf{h} \in \mathcal{R}^N$ are the known and the error (unknown) components of the PSF, respectively. The unknown component of the PSF is modeled as independent identically distributed (IID) noise, with zero-mean and variance σ_h^2. The justification for this assumption is twofold: first, it is the most generic model that one can use when no prior knowledge about the nature of the true PSF is available. Second, it simplifies the subsequent analysis of the proposed estimator.

The observation vector $\mathbf{g}$ is also subject to errors. We assume that $\mathbf{g}$ is contaminated by IID zero-mean additive noise with variance σ_g^2. Furthermore, the noises in the observed data and the PSF are assumed uncorrelated. Thus, the imaging equation in matrix-vector form is

$$\mathbf{g} = \mathbf{H}\mathbf{f} + \Delta\mathbf{g} \tag{2}$$

with

$$\mathbf{H} = \bar{\mathbf{H}} + \Delta\mathbf{H} \tag{3}$$

where $\mathbf{g}, \mathbf{f}, \Delta\mathbf{g} \in \mathcal{R}^N$ represent the observed degraded image, the source image and the additive noise in the observed image, respectively. $\bar{\mathbf{H}}$ is the known (assumed, estimated, or measured) component of the $N \times N$ PSF matrix $\mathbf{H}$, while $\Delta\mathbf{H}$ is the error component of the PSF matrix, made up by $\Delta\mathbf{h}$ from (1). For the rest of this paper circulant convolution of the PSF and the source image will be assumed, thus, $\mathbf{H}$ is an $N \times N$ circulant matrix [2] (for notational simplicity and without loss of generality circulant matrices instead of block-circulant matrices are used in the subsequent analysis). Linear convolution can always be performed using circular convolution after appropriate zero-padding of the convolved signals [2]. Since in most problems the support of the PSF is usually much smaller than the size of the image, this results in a very small change in the dimensions of the resulting matrices and vectors.

Equations (2) and (3) may be seen as a set of linear equations

$$\mathbf{g} \approx \mathbf{H}\mathbf{f} \tag{4}$$

where both $\mathbf{H}$ and $\mathbf{g}$ are subject to errors and the $\approx$ sign denotes that this set of linear equations cannot be solved exactly. Unless $\mathbf{g}$ belongs to the range of $\mathbf{H}$ ($R(\mathbf{H})$), the set of (4) has no exact solution and therefore, it can only be solved approximately.

TLS is a technique for solving linear equations as the ones in (4). The classical TLS formulation [7], [10] amounts to perturbing $\mathbf{H}$ and $\mathbf{g}$ by the necessary minimum quantities so as to make the set of (4) consistent. Mathematically, this can be expressed as

$$\min_{[\hat{\mathbf{H}}\,;\,\hat{\mathbf{g}}] \in \mathcal{R}^{N \times (N+1)}} \|[\mathbf{H}\,;\,\mathbf{g}] - [\hat{\mathbf{H}}\,;\,\hat{\mathbf{g}}]\|_F^2 \tag{5}$$

subject to

$$\hat{\mathbf{g}} \in R(\hat{\mathbf{H}}) \tag{6}$$

where

$$\|[\mathbf{H}\,;\,\mathbf{g}] - [\hat{\mathbf{H}}\,;\,\hat{\mathbf{g}}]\|_F = \|[\mathbf{\Delta H}\,;\,\mathbf{\Delta g}]\|_F \tag{7}$$

denotes the Frobenius norm of the matrix consisting of the columns of the matrix $\mathbf{\Delta H}$ and the vector $\mathbf{\Delta g}$. In other words, the norm of the residual of the PSF matrix and the observed data is minimized in a Frobenius sense. The Frobenius norm of an arbitrary $m \times n$ matrix $\mathbf{A}$ is defined as

$$\|\mathbf{A}\|_F = \sqrt{\sum_{i=1}^{m}\sum_{j=1}^{n} a_{ij}^2} = \sqrt{tr(\mathbf{A}^t\mathbf{A})} \tag{8}$$

where $tr(\cdot)$ denotes the trace of a matrix. Once a minimizer $[\hat{\mathbf{H}}\,;\,\hat{\mathbf{g}}]$ is found, any $\mathbf{f}$ satisfying $\hat{\mathbf{H}}\mathbf{f} = \hat{\mathbf{g}}$ is called a TLS solution and $[\mathbf{\Delta H}\,;\,\mathbf{\Delta g}]$ are the corresponding TLS corrections (residual) [7], [10].

In several instances the components of $\mathbf{\Delta H}$ may be algebraically related. This is the case when the blurring operator is circulant. Then, the error component of the PSF matrix $\mathbf{\Delta H}$ is also circulant. In this case, it is expedient both for computational and modeling purposes to represent $[\mathbf{\Delta H}\,;\,\mathbf{\Delta g}]$ in terms of a single vector that contains all the independent noise components [1]. Therefore, we define the unknown normalized noise vector $\mathbf{u} \in \mathcal{R}^{2N}$, consisting of $\mathbf{\Delta h}$ and $\mathbf{\Delta g}$, as follows

$$\mathbf{u} = \left[\frac{\Delta h(0)}{\sigma_h}, \cdots, \frac{\Delta h(N-1)}{\sigma_h}, \frac{\Delta g(0)}{\sigma_g}, \cdots, \frac{\Delta g(N-1)}{\sigma_g}\right]^t. \tag{9}$$

Here, the region of support for the noise part of the PSF is assumed to be N. However, if the region of support is M $(M < N)$, the remaining $N - M$ components would enter the noise vector $\mathbf{u}$ with zeros and the subsequent analysis would stay the same.

Since the noise perturbations in $\mathbf{H}$ come from a "common" noise source, $\mathbf{\Delta H}$ and $\mathbf{\Delta g}$ can be expressed as

$$\begin{aligned}\mathbf{\Delta H} &= [\mathbf{S}_0\mathbf{u}\ \ \mathbf{S}_1\mathbf{u}\ \cdots\ \mathbf{S}_{N-1}\mathbf{u}],\\ \mathbf{\Delta g} &= \mathbf{S}_N\mathbf{u}\end{aligned} \tag{10}$$

where the $\mathbf{S}_i$'s $(0 \le i \le N)$ are $N \times 2N$ noise dependency matrices and are determined by the "structure" of the application. It is straightforward to see that when $\mathbf{\Delta H}$ is circulant and $\mathbf{u}$ is defined by (9), the matrices $\mathbf{S}_i$ are given by

$$\mathbf{S}_0 = \begin{bmatrix} \sigma_h & 0 & 0 & \cdots & 0 & \vdots & 0 & 0 & \cdots & 0 & 0 \\ 0 & \sigma_h & 0 & \cdots & \vdots & \vdots & 0 & 0 & \cdots & 0 & 0 \\ 0 & 0 & \ddots & 0 & \vdots & \vdots & 0 & 0 & \cdots & 0 & 0 \\ \vdots & \vdots & 0 & \ddots & 0 & \vdots & 0 & 0 & \cdots & 0 & 0 \\ 0 & \cdots & \cdots & 0 & \sigma_h & \vdots & 0 & 0 & \cdots & 0 & 0 \end{bmatrix}$$

$$\mathbf{S}_1 = \begin{bmatrix} 0 & 0 & 0 & \cdots & \sigma_h & \vdots & 0 & 0 & \cdots & 0 & 0 \\ \sigma_h & 0 & \cdots & 0 & 0 & \vdots & 0 & 0 & \cdots & 0 & 0 \\ 0 & \sigma_h & 0 & \cdots & 0 & \vdots & 0 & 0 & \cdots & 0 & 0 \\ \vdots & 0 & \ddots & 0 & \vdots & \vdots & 0 & 0 & \cdots & 0 & 0 \\ 0 & \cdots & 0 & \sigma_h & 0 & \vdots & 0 & 0 & \cdots & 0 & 0 \end{bmatrix}$$

$$\vdots$$

$$\mathbf{S}_{N-1} = \begin{bmatrix} 0 & \sigma_h & 0 & \cdots & 0 & \vdots & 0 & 0 & \cdots & 0 & 0 \\ 0 & 0 & \sigma_h & 0 & \cdots & \vdots & 0 & 0 & \cdots & 0 & 0 \\ 0 & 0 & 0 & \ddots & 0 & \vdots & 0 & 0 & \cdots & 0 & 0 \\ \vdots & \vdots & \vdots & 0 & \sigma_h & \vdots & 0 & 0 & \cdots & 0 & 0 \\ \sigma_h & 0 & \cdots & 0 & 0 & \vdots & 0 & 0 & \cdots & 0 & 0 \end{bmatrix}$$

and

$$\mathbf{S}_N = \begin{bmatrix} 0 & 0 & \cdots & 0 & 0 & \vdots & \sigma_g & 0 & \cdots & 0 & 0 \\ 0 & 0 & \cdots & 0 & 0 & \vdots & 0 & \sigma_g & 0 & 0 & 0 \\ 0 & 0 & \cdots & 0 & 0 & \vdots & 0 & 0 & \ddots & 0 & \cdots \\ \vdots & \vdots & \cdots & \vdots & \vdots & \vdots & \vdots & \vdots & 0 & \ddots & 0 \\ 0 & 0 & \cdots & 0 & 0 & \vdots & 0 & 0 & \cdots & 0 & \sigma_g \end{bmatrix}. \tag{11}$$

Substituting (10) into the functional of (5), we obtain

$$\begin{aligned}\|[\mathbf{\Delta H}\,;\,\mathbf{\Delta g}]\|_F^2 &= \|[\mathbf{S}_0\mathbf{u}\ \ \mathbf{S}_1\mathbf{u}\ \cdots\ \mathbf{S}_{N-1}\mathbf{u}\ \ \mathbf{S}_N\mathbf{u}]\|_F^2\\ &= \textstyle\sum_{i=0}^{N} \|\mathbf{S}_i\,\mathbf{u}\|_2^2\end{aligned} \tag{12}$$

where $\|\cdot\|_2$ denotes the Euclidean norm. From previous definitions, it is easy to see that

$$\|\mathbf{S}_i\,\mathbf{u}\|_2^2 = \sum_{j=0}^{N-1} \Delta h^2(j)\,,\ \ \forall i = 0, 1, \cdots, N-1. \tag{13}$$

We can therefore write

$$\sum_{i=0}^{N} \|\mathbf{S}_i\,\mathbf{u}\|_2^2 = \sum_{j=0}^{N-1} (N\Delta h^2(j) + \Delta g^2(j)) = \mathbf{u}^t\mathbf{W}\,\mathbf{u} \tag{14}$$

where $\mathbf{W}$ is a $2N \times 2N$ diagonal matrix given by

$$\mathbf{W} = \text{diag}\,[N{\sigma_h}^2, \cdots, N{\sigma_h}^2, {\sigma_g}^2, \cdots, {\sigma_g}^2]. \tag{15}$$

A similar CTLS functional as in (14) was derived in [1] assuming the same statistical properties of the noise in $\mathbf{H}$ and $\mathbf{g}$. In [1], it was also shown that using a Gaussian setting the CTLS estimate is equivalent to a ML estimate. In our formulation, it is easy to see that the functional in (14) does not take into consideration the variance of the noise in $\mathbf{H}$ and $\mathbf{g}$. Therefore, for our CTLS formulation instead of minimizing the functional $\mathbf{u}^t\mathbf{W}\,\mathbf{u}$, we minimize $\mathbf{u}^t\mathbf{u} = \|\mathbf{u}\|_2{}^2$. By defining a proper norm to weight all noise components equally, we minimize $\mathbf{u}^t\mathbf{u} = \|\mathbf{u}\|_2{}^2$ and preserve the equivalency between our CTLS estimator and a ML one. This guarantees that our CTLS estimator has a number of desirable properties as the

one in [1] (minimum variance among unbiased estimators and asymptotic efficiency [14], among others).

Equations (2) and (3) can be reformulated as follows:

$$\bar{\mathbf{H}}\mathbf{f} - \mathbf{g} + \Delta\mathbf{H}\mathbf{f} + \Delta\mathbf{g} = 0$$

$$\bar{\mathbf{H}}\mathbf{f} - \mathbf{g} + \left(\sum_{i=0}^{N-1} f(i)\mathbf{S}_i + \mathbf{S}_N\right)\mathbf{u} = 0 \tag{16}$$

$$\bar{\mathbf{H}}\mathbf{f} - \mathbf{g} + \mathbf{L}\,\mathbf{u} = 0$$

where

$$\mathbf{L} = \left(\sum_{i=0}^{N-1} f(i)\mathbf{S}_i\right) + \mathbf{S}_N \tag{17}$$

is the $N \times 2N$ matrix with circulant structure, given below

$$\left[\begin{array}{cccc:c} \sigma_h f(0) & \sigma_h f(N-1) & \cdots & \sigma_h f(1) & \vdots & \\ \sigma_h f(1) & \sigma_h f(0) & \cdots & \sigma_h f(2) & \vdots & \\ \sigma_h f(2) & \sigma_h f(1) & \cdots & \sigma_h f(3) & \vdots & \sigma_g \mathbf{I}_{\mathbf{N}\times\mathbf{N}} \\ \vdots & \vdots & \ddots & \vdots & \vdots & \\ \sigma_h f(N-1) & \sigma_h f(N-2) & \cdots & \sigma_h f(0) & \vdots & \end{array}\right]. \tag{18}$$

Accordingly, the CTLS image restoration problem can be rephrased as

$$\min_{\mathbf{f}} \{\|\mathbf{u}\|_2^2\} \tag{19}$$

subject to

$$\bar{\mathbf{H}}\mathbf{f} - \mathbf{g} + \mathbf{L}\,\mathbf{u} = \mathbf{0}. \tag{20}$$

III. Regularized Constrained Total Least Squares Image Restoration

The determination of the source function $\mathbf{f}$ in (2), given the recorded data $\mathbf{g}$ and knowledge of the PSF is an inverse problem. The solution of the image restoration problem corresponds mathematically to the existence and uniqueness of an inverse transformation of (2). If the inverse transformation does not exist, then there is no mathematical basis for recovering $\mathbf{f}$ from $\mathbf{g}$, but there may be a practical basis for asserting that something very close to $\mathbf{f}$ can be recovered. Problems for which there is no inverse transformation are said to be singular. On the other hand, an inverse transformation may exist but not be unique. Finally, even if the inverse transformation exists and is unique, it is ill-conditioned, meaning that trivial perturbations in $\mathbf{g}$ can produce nontrivial perturbations in $\mathbf{f}$ [20], [2]. Therefore, one must select the proper solution from an infinite family of candidate solutions. The proper solution is usually derived from various combinations of available prior information about the estimated signal and appropriate criteria of performance in the solution.

One of the most powerful approaches to overcome these difficulties in ill-posed problems is regularization [20], [4]. According to this approach, to select the proper solution, recorded data and *a priori* knowledge are used in a complementary way [11], [6]. In [6] the least-squares (LS) and the RLS restored images were compared when $\mathbf{H}$ is exactly known. It was rigorously shown that the RLS estimate is a better estimate than the LS estimate, based on the MSE criterion. Motivated by this, we propose next the RCTLS formulation. In Section IV, this choice is mathematically justified.

According to the regularization approach the minimization in (19) is replaced by the minimization of

$$\min_{\mathbf{f}} \{\|\mathbf{u}\|_2^2 + \lambda \|\mathbf{Q}\,\mathbf{f}\|_2^2\} \tag{21}$$

subject to

$$\bar{\mathbf{H}}\mathbf{f} - \mathbf{g} + \mathbf{L}\,\mathbf{u} = \mathbf{0} \tag{22}$$

where $\mathbf{Q}$ is the regularization operator and λ is a positive parameter known as the regularization parameter [11]. Equation (21) has the same physical foundation as the ordinary RLS, introduced for the first time in [11] and used widely thereafter. The role of the regularization operator is to incorporate prior knowledge about $\mathbf{f}$ into the restoration process (see for example [11], [4], [6]). The smoothness of $\mathbf{f}$ is the prior knowledge on which the selection of $\mathbf{Q}$ is usually based.

The addition of the regularization term to (19) can also be viewed as converting an ML estimation problem to a MAP one, when a Gaussian setting is assumed [4], [17]. In this context, $\mathbf{Q}^t\mathbf{Q}$ plays the role of the inverse covariance of the assumed prior distribution (see for example [4], [6]). Therefore, the problem of finding a good regularization operator and good regularization parameter can be replaced by estimating the covariance matrix (or power spectrum in the DFT domain) of the source signal.

Equation (21) represents a quadratic minimization problem that is subject to a nonlinear constraint due to the term $\mathbf{L}\,\mathbf{u}$ in (22). A closed form solution may not exist. However, the RCTLS problem in (21) and (22) can be further simplified by transforming it into an unconstrained optimization problem. First, (22) is rewritten as

$$\mathbf{L}\,\mathbf{u} = -(\bar{\mathbf{H}}\mathbf{f} - \mathbf{g}) \tag{23}$$

then

$$\mathbf{u} = -\mathbf{L}^{\dagger}(\bar{\mathbf{H}}\mathbf{f} - \mathbf{g}) \tag{24}$$

where $\mathbf{L}^{\dagger}$ is the Moore–Penrose pseudoinverse of $\mathbf{L}$ [8]. It is easy to see from (18) that matrix $\mathbf{L}$ has rank N, therefore $\mathbf{L}^{\dagger}$ is given by

$$\mathbf{L}^{\dagger} = \mathbf{L}^{\mathbf{t}}(\mathbf{L}\,\mathbf{L}^{\mathbf{t}})^{-1}. \tag{25}$$

Substituting (24) into (21), the RCTLS formulation in (21) and (22) is equivalent to minimizing a nonlinear function $P(\mathbf{f})$ with respect to $\mathbf{f}$, where $P(\mathbf{f})$ is defined as

$$P(\mathbf{f}) = (\bar{\mathbf{H}}\mathbf{f} - \mathbf{g})^{\mathbf{t}}(\mathbf{L}^{\dagger})^{\mathbf{t}}(\mathbf{L}^{\dagger})(\bar{\mathbf{H}}\mathbf{f} - \mathbf{g}) + \lambda(\mathbf{f}^{\mathbf{t}}\mathbf{Q}^{\mathbf{t}}\mathbf{Q}\,\mathbf{f}). \tag{26}$$

The above equation can be further simplified, noting that

$$(\mathbf{L}^{\dagger})^{\mathbf{t}}(\mathbf{L}^{\dagger}) = (\mathbf{L}\,\mathbf{L}^{\mathbf{t}})^{-1} \tag{27}$$

to obtain

$$P(\mathbf{f}) = (\bar{\mathbf{H}}\mathbf{f} - \mathbf{g})^{\mathbf{t}}(\mathbf{L}\,\mathbf{L}^{\mathbf{t}})^{-1}(\bar{\mathbf{H}}\mathbf{f} - \mathbf{g}) + \lambda(\mathbf{f}^{\mathbf{t}}\mathbf{Q}^{\mathbf{t}}\mathbf{Q}\,\mathbf{f}). \tag{28}$$

Equation (28) represents the transformation of the constrained minimization problem, in (21) and (22), into an

unconstrained one. Hence, the RCTLS solution of (21) and (22) can be obtained by minimizing $P(\mathbf{f})$ with respect to $\mathbf{f}$. It may not be possible to find the minimum of (28) in closed form because of the nonlinearity in the term $(\mathbf{L}\,\mathbf{L}^t)^{-1}$. However, it is possible to obtain a solution numerically by iterative optimization algorithms. For average size images the computations required for the minimization of $P(\mathbf{f})$ in (28) is prohibitively large. For example, if a 256×256 gray-scale image is processed, the matrices in (28) would be of size $65\,536 \times 65\,536$, which is unrealistic to handle with the present computer technology. Furthermore, $P(\mathbf{f})$ is a nonconvex function that makes this optimization even harder.

Equation (28) can be further simplified in the DFT domain. In Appendix A, we show that the minimization of $P(\mathbf{f})$ in (28) is equivalent to

$$\min_{F(i)} \{P(F(i))\}\ ,\ \text{for } i = 0, 1, \cdots, N-1 \tag{29}$$

where the $P(F(i))$ are given by

$$P(F(i)) = \frac{|\bar{H}(i)F(i) - G(i)|^2}{{\sigma_h}^2|F(i)|^2 + {\sigma_g}^2} + \lambda\,|Q(i)|^2|F(i)|^2 \tag{30}$$

and $|\cdot|$ denotes the modulus of a complex quantity. $F(i)$ and $G(i)$ are the DFT coefficients of the corresponding lower case spatial-domain quantities. $\bar{H}(i)$ and $Q(i)$ are the eigenvalues of the circulant matrices $\bar{\mathbf{H}}$ and $\mathbf{Q}$, which can be easily obtained using the DFT [2]. The resulting computational simplification is obvious. Equation (28) is decoupled into N equations, each to be minimized independently with respect to one DFT coefficient of $\mathbf{f}$. Each of these equations still requires solving a vector optimization problem. However, the dimensionality of the problem has been reduced to two, the real and the imaginary part of the complex DFT coefficient $F(i)$. From (30), it is clear that when the variance of the noise in the PSF ${\sigma_h}^2$ becomes zero, the RCTLS estimate degenerates, as expected, to the RLS estimate [6]. In that case, the PSF matrix $\bar{\mathbf{H}}$ coincides with $\mathbf{H}$ and the regularization parameter λ_{RLS} is equal to ${\sigma_g}^2\lambda_{RCTLS}$.

IV. Perturbation Analysis of the RCTLS Estimator

Due to the nonlinear character of the RCTLS problem, the error analysis of the RCTLS estimator appears to be an intractable problem. Therefore, we resort to a perturbation analysis [1], [5], [7] to derive an analytic formula for the MSE of the RCTLS estimate. The necessary condition for a minimum of (28) is that its gradient is equal to zero. Setting the gradient of $P(\mathbf{f})$ given in (28) with respect to $\mathbf{f}$, equal to zero, yields

$$\begin{aligned}\frac{\partial P(\mathbf{f})}{\partial \mathbf{f}} &= 2[\bar{\mathbf{H}}^t - (\bar{\mathbf{H}}\mathbf{f} - \mathbf{g})^t(\mathbf{L}\mathbf{L}^t)^{-1}\\ &\frac{1}{4}(\frac{\partial \boldsymbol{L}}{\partial \boldsymbol{f}}\mathbf{L}^t + \mathbf{L}\frac{\partial \mathbf{L}^t}{\partial \mathbf{f}})](\mathbf{L}\mathbf{L}^t)^{-1}(\bar{\mathbf{H}}\mathbf{f} - \mathbf{g})\\ &+ 2\,\lambda\mathbf{Q}^t\mathbf{Q}\,\mathbf{f} = \mathbf{0}.\end{aligned} \tag{31}$$

Observe that (2) can be rewritten as

$$\mathbf{g} = \bar{\mathbf{g}} + \boldsymbol{\Delta}\tilde{\mathbf{g}} \tag{32}$$

where

$$\bar{\mathbf{g}} = \bar{\mathbf{H}}\,\mathbf{f} \tag{33}$$

and

$$\boldsymbol{\Delta}\tilde{\mathbf{g}} = \boldsymbol{\Delta}\mathbf{H}\,\mathbf{f} + \boldsymbol{\Delta}\mathbf{g}. \tag{34}$$

Now, suppose that the unperturbed (noise-free) system of linear equations $\bar{\mathbf{H}}\,\mathbf{f} = \bar{\mathbf{g}}$ has a consistent solution $\mathbf{f}_0$. Perturb $\bar{\mathbf{g}}$ by $\boldsymbol{\Delta}\tilde{\mathbf{g}}$ to $\mathbf{g} = \bar{\mathbf{g}} + \boldsymbol{\Delta}\tilde{\mathbf{g}}$ around the consistent solution $\mathbf{f}_0$. Then, the consistent solution $\mathbf{f}_0$ is perturbed by $\boldsymbol{\Delta}\mathbf{f}$, where $\boldsymbol{\Delta}\mathbf{f}$ is caused by $\boldsymbol{\Delta}\mathbf{H}$ and $\boldsymbol{\Delta}\mathbf{g}$. The perturbation error$\boldsymbol{\Delta}\mathbf{f}$ is what we really want to obtain analytically and to analyze statistically in terms of its bias and covariance. Using $\bar{\mathbf{H}}\,\mathbf{f}_0 = \bar{\mathbf{g}}$ and neglecting higher order terms in $\boldsymbol{\Delta}\mathbf{f}, \boldsymbol{\Delta}\mathbf{H}$, $\boldsymbol{\Delta}\mathbf{g}$, and their crossproducts, we obtain from (31) that

$$\begin{aligned}\frac{\partial P(\mathbf{f})}{\partial \mathbf{f}} = \mathbf{0} \Longleftrightarrow\ &\bar{\mathbf{H}}^t(\mathbf{L}_0\mathbf{L}_0{}^t)^{-1}(\bar{\mathbf{H}}\boldsymbol{\Delta}\mathbf{f} - \boldsymbol{\Delta}\mathbf{H}\mathbf{f}_0 - \boldsymbol{\Delta}\mathbf{g})\\ &+\lambda\mathbf{Q}^t\mathbf{Q}(\mathbf{f}_0 + \boldsymbol{\Delta}\mathbf{f}) = \mathbf{0}\end{aligned} \tag{35}$$

where $\mathbf{L}_0$ is the same as in (18), and contains the elements of the consistent solution $\mathbf{f}_0$. Let

$$\mathbf{A} = \bar{\mathbf{H}}^t(\mathbf{L}_0\,\mathbf{L}_0{}^t)^{-1}. \tag{36}$$

Solving (35) for $\boldsymbol{\Delta}\mathbf{f}$, we obtain

$$\boldsymbol{\Delta}\mathbf{f} = (\mathbf{A}\,\bar{\mathbf{H}} + \lambda\,\mathbf{Q}^t\mathbf{Q})^{-1}\left[\mathbf{A}\,(\boldsymbol{\Delta}\mathbf{H}\,\mathbf{f}_0 + \boldsymbol{\Delta}\mathbf{g}) - \lambda\,\mathbf{Q}^t\mathbf{Q}\,\mathbf{f}_0\right]. \tag{37}$$

From (16), it is easy to see that

$$\boldsymbol{\Delta}\mathbf{H}\,\mathbf{f}_0 + \boldsymbol{\Delta}\mathbf{g} = \mathbf{L}_0\mathbf{u}. \tag{38}$$

Substituting (38) into (37), we finally get

$$\boldsymbol{\Delta}\mathbf{f} = (\mathbf{A}\,\bar{\mathbf{H}} + \lambda\,\mathbf{Q}^t\mathbf{Q})^{-1}\left\{\mathbf{A}\,\mathbf{L}_0\,\mathbf{u} - \lambda\,\mathbf{Q}^t\mathbf{Q}\,\mathbf{f}_0\right\}. \tag{39}$$

Equation (39) is a closed-form expression of the perturbation from the consistent solution of the RCTLS estimate. Since it was derived by neglecting higher order terms in $\boldsymbol{\Delta}\mathbf{f}$, $\boldsymbol{\Delta}\mathbf{H}$, $\boldsymbol{\Delta}\mathbf{g}$, and their crossproducts it is valid for small noise levels.

Next, we proceed to find the MSE of the RCTLS estimate. Let

$$\varepsilon = E\{\|\mathbf{f} - \mathbf{f}_0\|^2\} = E\{\|\boldsymbol{\Delta}\mathbf{f}\|^2\} \tag{40}$$

be the MSE of the RCTLS estimate, where E is the expectation operator. Then, (40) can be expressed as

$$\varepsilon = tr[\mathbf{C}] + tr[\mathbf{b}\,\mathbf{b}^t] \tag{41}$$

where $\mathbf{C}$ and $\mathbf{b}$ are the covariance matrix of the random vector $\boldsymbol{\Delta}\mathbf{f}$ and its bias, respectively. More specifically,

$$\mathbf{b} = E\{\mathbf{f}\} - \mathbf{f}_0 = E\{\mathbf{f}_0 + \boldsymbol{\Delta}\mathbf{f}\} - \mathbf{f}_0 = E\{\boldsymbol{\Delta}\mathbf{f}\} \tag{42}$$

and

$$\mathbf{C} = E\{\boldsymbol{\Delta}\mathbf{f}\,\boldsymbol{\Delta}\mathbf{f}^t\} - E\{\boldsymbol{\Delta}\mathbf{f}\}E\{\boldsymbol{\Delta}\mathbf{f}^t\}. \tag{43}$$

Since the noise vector $\mathbf{u}$ is assumed to be zero-mean, it is easy to see from (39) and (42), that the MSE of the CTLS estimate ($\lambda = 0$) consists of the variance part given by $tr(\mathbf{C})$ only. Thus, the CTLS estimate is unbiased.

Using the diagonalization properties of the DFT for the circulant matrices $\bar{\mathbf{H}}$, $\mathbf{Q}$ and $\mathbf{L_0}$, we show in Appendix B that in the DFT domain

$$tr[\mathbf{b}\,\mathbf{b}^t] = \sum_{i=0}^{N-1} \frac{\lambda^2 |Q(i)|^4 |F_0(i)|^2}{\left[\frac{|\bar{H}(i)|^2}{{\sigma_h}^2 |F_0(i)|^2 + {\sigma_g}^2} + \lambda |Q(i)|^2\right]^2} \tag{44}$$

where $Q(i), F_0(i)$ and $\bar{H}(i)$ are given similarly as in (30). We also show in Appendix B that $tr[\mathbf{b}\,\mathbf{b}^t]$ is a strictly positive monotonically increasing function of λ, for $\lambda > 0$. Furthermore, it is easy to see from (44) that

$$tr[\mathbf{b}\,\mathbf{b}^t(\lambda \to 0)] = 0 \tag{45}$$

and

$$tr[\mathbf{b}\,\mathbf{b}^t(\lambda \to \infty)] = \sum_{i=0}^{N-1} |F_0(i)|^2 = \|\mathbf{f_0}\|^2. \tag{46}$$

Similarly, in Appendix B we show that in the DFT domain, the variance can be expressed as

$$tr[\mathbf{C}] = \sum_{i=0}^{N-1} \frac{\frac{|\bar{H}(i)|^2}{{\sigma_h}^2 |F_0(i)|^2 + {\sigma_g}^2}}{\left[\frac{|\bar{H}(i)|^2}{{\sigma_h}^2 |F_0(i)|^2 + {\sigma_g}^2} + \lambda |Q(i)|^2\right]^2}. \tag{47}$$

We also show in Appendix B that $tr[\mathbf{C}]$ is a strictly positive, monotonically decreasing function of λ, for $\lambda > 0$. Furthermore, from (47)

$$tr[\mathbf{C}(\lambda \to \infty)] = 0 \tag{48}$$

and

$$tr[\mathbf{C}(\lambda \to 0)] = \sum_{i=0}^{N-1} \frac{{\sigma_h}^2 |F_0(i)|^2 + {\sigma_g}^2}{|\bar{H}(i)|^2}. \tag{49}$$

Therefore, the total MSE error as a function of λ is a sum of a monotonically decreasing and a monotonically increasing function of λ. Examining the first and second derivatives of ε, with respect to λ, we show in Appendix B that the MSE of the RCTLS estimate is a monotonically decreasing function for

$$0 \leq \lambda < \left(\frac{1}{|Q(i)|^2 |F_0(i)|^2}\right)_{min} \tag{50}$$

and a monotonically increasing function for

$$\left(\frac{1}{|Q(i)|^2 |F_0(i)|^2}\right)_{max} \leq \lambda < \infty \tag{51}$$

where $(\cdot)_{min}$ and $(\cdot)_{max}$ denote the minimum and maximum of the expressions inside the parenthesis with respect to i.

Furthermore, we show that the MSE as a function of λ has a minimum for $0 \leq \lambda < \infty$, which lies in the interval

$$\left[\left(\frac{1}{|Q(i)|^2 |F_0(i)|^2}\right)_{min}, \left(\frac{1}{2|Q(i)|^2} \frac{|\bar{H}(i)|^2}{{\sigma_h}^2 |F_0(i)|^2 + {\sigma_g}^2} + \frac{3}{2} \frac{1}{|Q(i)|^2 |F_0(i)|^2}\right)_{min}\right]. \tag{52}$$

It is interesting to note that (44), (47), (50), and (51) are generalizations of the equations obtained in [6], in the error analysis of the LS, and the RLS estimators. More specifically, for the case when ${\sigma_h}^2 = 0$ and after replacing parameter λ_{RCTLS} by $\frac{\lambda_{RLS}}{\sigma_g^2}$ in (44), (47), (50), and (51), the bias, the covariance, and the lower and upper bounds for λ_{RLS} of the RLS estimator in [6] are obtained, respectively.

We denote the value of λ where the minimum error occurs as λ_{mse}. Then, ε is a decreasing function for $0 \leq \lambda \leq \lambda_{mse}$ and an increasing function for $\lambda_{mse} \leq \lambda < \infty$. Thus, for any λ in $0 \leq \lambda \leq \lambda_{mse}$, we have $\varepsilon_{RCTLS} < \varepsilon_{CTLS}$. Furthermore, $\bar{\mathbf{H}}$ in many applications has some eigenvalues close to zero. In this case, from (46) and (49) we get that $tr[\mathbf{C}(\lambda \to 0)] > tr[\mathbf{b}\mathbf{b}^t(\lambda \to \infty)]$ which implies that for $0 \leq \lambda < \infty$, we have $\varepsilon_{RCTLS} < \varepsilon_{CTLS}$.

From the discussion in the previous paragraph it is clear that the RCTLS estimate is in general a better estimate than the CTLS one in the MSE sense. Obviously, the bias introduced by the regularization term in (21) was a price well worth paying, since it reduced the total MSE. Similar observations were made in [6], where the MSE of the LS and RLS estimates were compared, and the results obtained there are the special case of the ones derived here.

V. Numerical Experiments

In this section, numerical experiments are presented to test the proposed restoration algorithm. The RCTLS approach is compared to the LMMSE and the RLS approaches. The LMMSE filter used for this comparison has been reformulated to include the errors in the PSF as additive signal-dependent noise [21], [9]. Starting from (2), it is easy to show that in the DFT domain, for circulant $\bar{\mathbf{H}}$ and autocorrelation matrix $\mathbf{R_f} = E\{\mathbf{f}\,\mathbf{f}^t\}$, the modified LMMSE (Wiener) estimate of $\mathbf{f}$ is given by

$$\hat{F}(i) = \frac{\bar{H}^*(i)G(i)}{|\bar{H}(i)|^2 + \frac{{\sigma_h}^2 S_{ff}(i) + {\sigma_g}^2}{S_{ff}(i)}}, i = 0, 1, \cdots, N-1 \tag{53}$$

where the $S_{ff}(i)$ are the power spectrum coefficients (eigenvalues of $\mathbf{R_f}$) of the source image. To estimate the $S_{ff}(i)$ we used the periodogram of the source image. Furthermore, to achieve better results, we regularized the LMMSE estimate [2] as follows:

$$\hat{F}(i) = \frac{\bar{H}^*(i)G(i)}{|\bar{H}(i)|^2 + \lambda_{LMMSE} \frac{{\sigma_h}^2 S_{ff}(i) + {\sigma_g}^2}{S_{ff}(i)}} \tag{54}$$

where λ_{LMMSE} was computed using the source image to yield the minimum MSE for $0 \leq \lambda_{LMMSE} < \infty$. In other words, in all our experiments we compared the RCTLS estimate with the *best possible* LMMSE estimate, based on the knowledge of the source image.

The RCTLS and the RLS filters necessitate the determination of the regularization parameter λ and the regularization operator $\mathbf{Q}$. The Laplacian operator was used as the regularization operator [6], for both methods. For comparison purposes for the RLS filter, we used the optimal λ in the MSE sense that was computed using the source image. In all our experiments the same value of ${\sigma_h}^2$ was supplied to both LMMSE and RCTLS filters. For the RCTLS filter, the parameter λ was selected by a trial and error approach, without knowledge

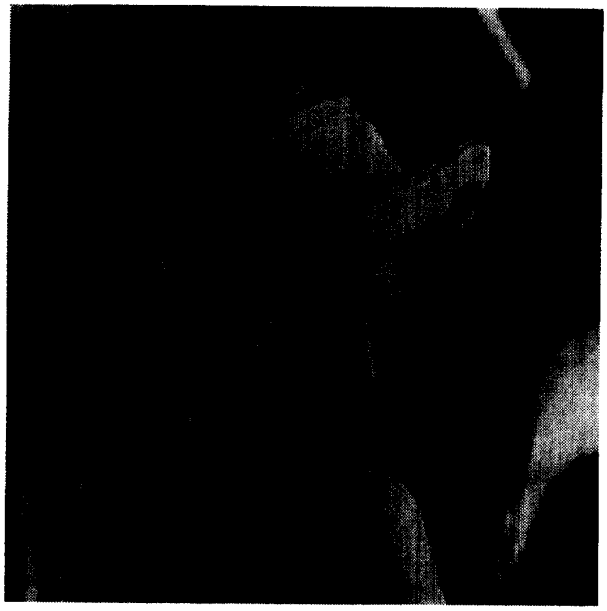

Fig. 1. Original "Lena" 256 × 256 image

of the source image, based only on visual inspection of the results.

As objective measure of performance, the improvement in signal-to-noise-ratio (ISNR) was used. It is defined by

$$ISNR = 20 \log \frac{\|\mathbf{f} - \mathbf{g}\|_2}{\|\mathbf{f} - \hat{\mathbf{f}}\|_2} \tag{55}$$

where $\mathbf{f}$, $\mathbf{g}$ and $\hat{\mathbf{f}}$ are the original, degraded, and estimated signals, respectively.

For the blur, in all experiments presented in this paper we used a Gaussian-shaped PSF, which is given by

$$h(i,j) = c \exp\left\{-\frac{i^2+j^2}{2\sigma^2}\right\}, \text{ for } i,j = 0,1,\cdots,N-1 \tag{56}$$

where c is a constant that ensures a lossless response system, i.e.

$$\sum_{i,j} h(i,j) = 1. \tag{57}$$

In what follows, we present three experiments where different types of approximations of the true PSF were used to test the proposed method. More experiments can be found in [15]. The 256 × 256 "Lena" image, shown in Fig. 1, was used as a source image.

Experiment 1: In this experiment, the Gaussian-shaped PSF used to blur the source image had variance $\sigma^2 = 6.25$. The PSF used for restoration by all three filters was the previous one corrupted with additive white Gaussian noise of variance $\sigma_h{}^2 = 8 \cdot 10^{-7}$. For both PSF's, the region of support was 29 × 29 pixels. Gaussian noise with $\sigma_g{}^2 = 1.0$ was used as $\Delta\mathbf{g}$. The corresponding ISNR values for this experiment are given in Table I. The degraded and restored images with the LMMSE, RLS, and RCTLS methods are shown in Fig. 2(a), 2(b), 2(c), and 2(d), respectively.

TABLE I
ISNR RESULTS FOR EXPERIMENT 1

		ISNR [dB]		
$\sigma_h{}^2$	$\sigma_g{}^2$	LMMSE	RLS	RCTLS
$8.0 \cdot 10^{-7}$	1.0	-2.05	-2.12	1.17

TABLE II
ISNR RESULTS FOR EXPERIMENT 2

		ISNR [dB]		
$\sigma_h{}^2$	$\sigma_g{}^2$	LMMSE	RLS	RCTLS
$2.3 \cdot 10^{-6}$	0.1	-0.77	-1.04	2.52

TABLE III
ISNR RESULTS FOR EXPERIMENT 3

		ISNR [dB]		
$\sigma_h{}^2$	$\sigma_g{}^2$	LMMSE	RLS	RCTLS
$5.2 \cdot 10^{-8}$	1.0	-1.10	-0.98	2.45

Experiment 2: In this experiment, we assumed that the variance σ^2 of the Gaussian-shaped PSF is incorrectly known. The PSF used to blur the source image had $\sigma^2 = 9$, while the PSF used by all three restoration filters had $\sigma^2 = 16$. For both PSF's the region of support was 31 × 31 pixels. Additive white Gaussian noise with variance $\sigma_g{}^2 = 0.1$ was used as $\Delta\mathbf{g}$. Using the notation in (1) the true PSF used to blur the signal is $\mathbf{h}$ and the erroneous one used for restoration is $\bar{\mathbf{h}}$. The difference $\mathbf{h} - \bar{\mathbf{h}} = \Delta\mathbf{h}$ is the error due to inexact knowledge of the PSF. The corresponding ISNR values for this experiment are given in Table II. The degraded and restored images with the LMMSE, RLS, and RCTLS methods are shown in Fig. 3(a), 3(b), 3(c), and 3(d), respectively.

Experiment 3: A Gaussian-shaped PSF extending over 17 × 17 pixels with variance $\sigma^2 = 4$ and additive Gaussian noise with variance $\sigma_g^2 = 1.0$ was used to degrade the original image. A 2-D linear approximation of the Gaussian-shaped PSF was used for restoration by all three filters. The projections of the equiheight lines of the true and assumed erroneous PSF are shown in Fig. 4. The ISNR values for this experiment are given in Table III. Degraded and restored images using the LMMSE, RLS, and RCTLS filters, are shown in Fig. 5(a)–(d), respectively.

From our experiments, we observe that the RCTLS method, even though it did not use the knowledge of the source image as for the LMMSE filter and to a less extent for the RLS filter, outperformed both of them both visually and objectively based on the ISNR metric. In addition, we observed that the RCTLS filter outperformed more decisively the LMMSE and the RLS filters around the image edges. Furthermore, this difference was more pronounced when the error in the PSF was systematic rather than random. Our explanation for these observations is based on the fact that random errors in the PSF tend to average out in smooth areas of the image. Thus, the errors in the observed data are bigger around the edges, rather than in the smooth areas of the image. Furthermore, the errors in the observed data are, in general,

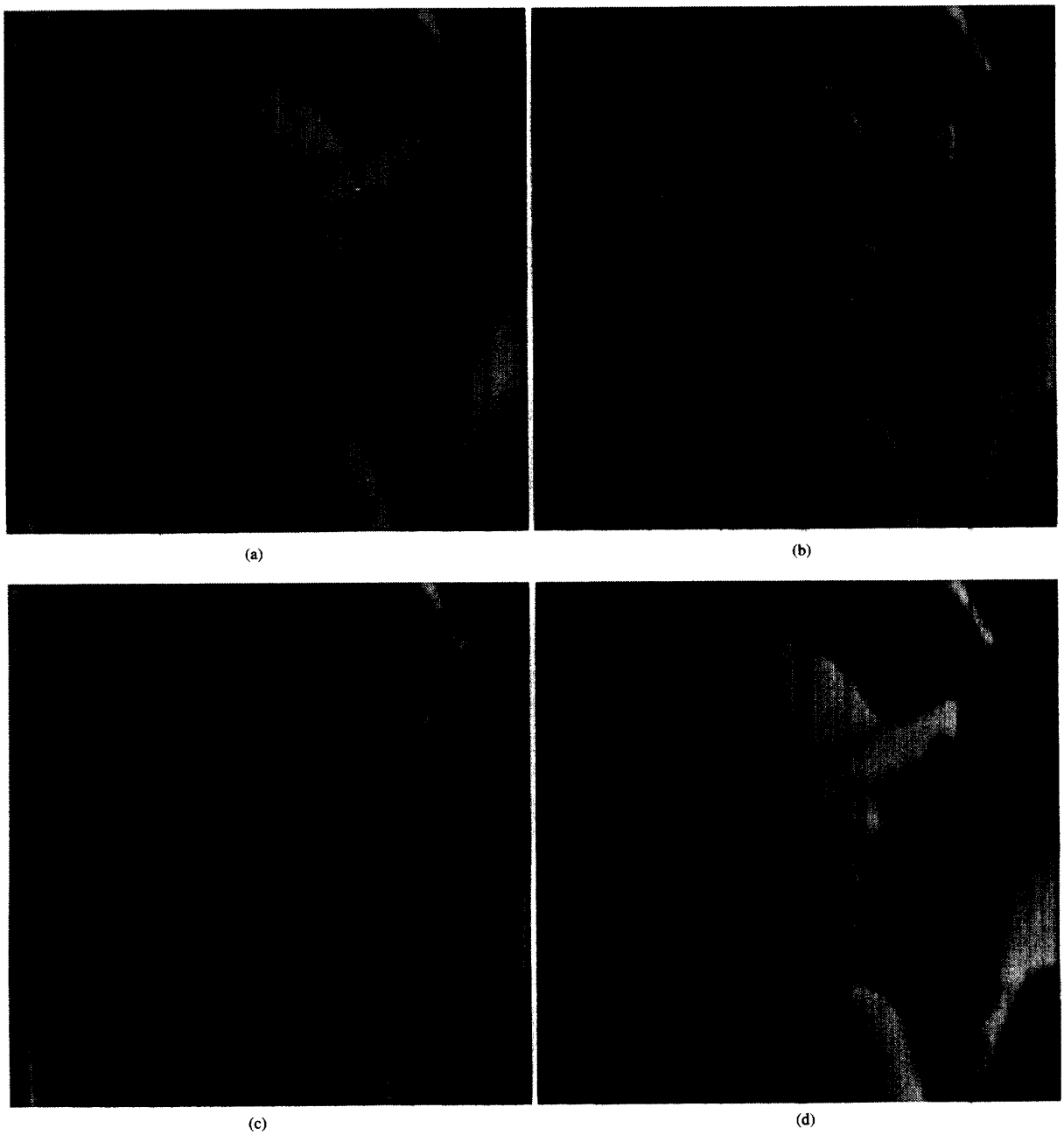

Fig. 2. Experiment 1. (a) Degraded image; (b) LMMSE estimate; (c) RLS estimate; (d) RCTLS estimate.

bigger in cases of systematic rather than random errors in the PSF.

For the implementation of the RCTLS filter, we minimized (30) with respect to the real and the imaginary parts of $F(i)$ for every discrete frequency i, using the Davidon–Fletcher–Powell optimization algorithm in [16]. The gradient required by this algorithm was found in closed form. As a starting point for this algorithm we used the degraded signal and for every frequency the algorithm converged in less than five iterations. For a $256\times$ 256 gray-scale image the computation of the RCTLS estimator required one-two minutes on a SUN-SPARC10 workstation, thus, requiring overall two-three times more time than the other two methods. Because of the nonconvex nature of $P(F(i))$ in (30), we used a number of initial conditions (the source image, the degraded and the restored images by the LMMSE and the RLS filters) to test the point of convergence of our algorithm. In all cases, we found that this selection did not alter the convergence point of our algorithm.

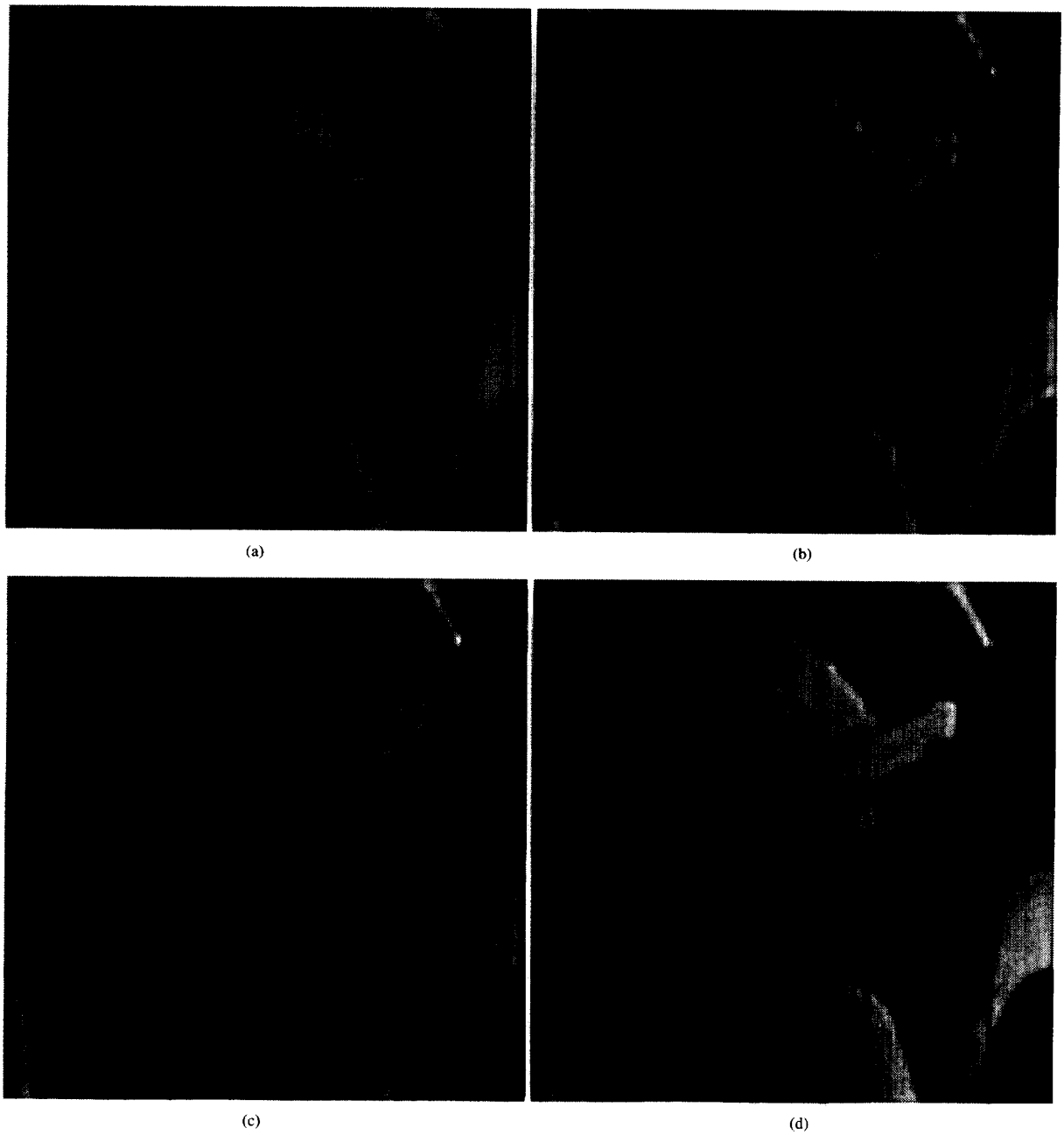

Fig. 3. Experiment 2 (a) Degraded image; (b) LMMSE estimate; (c) RLS estimate; (d) RCTLS estimate.

VI. Conclusions

In this paper, we introduced a regularized constrained total least-squares (RCTLS) formulation of the image restoration problem, when the point-spread function (PSF) is not known accurately. Using the diagonalization properties of the discrete Fourier transform (DFT), we derived the RCTLS estimate in the DFT domain, thus, making possible its implementation for large images. We performed a perturbation analysis of this estimate and showed its advantages over the CTLS one. As a special case of the perturbation analysis in this paper, we obtained the mean-squared-error (MSE) analysis of the regularized least-squares (RLS) estimator [6]. In all our experiments, both in this paper and in [15], the proposed approach showed the ability to outperform both the RLS and the LMMSE estimates. In the case of systematic PSF error the RCTLS approach outperformed dramatically the other two methods based on both objective MSE-based metrics and subjective visual criteria. For the RLS filter, since no provision was made in the restoration algorithm to include

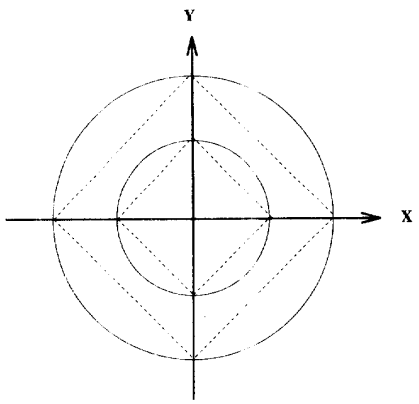

Fig. 4. Experiment 3. Equivalue lines for the 2-D PSF; exact PSF (solid) and its linear approximation (dashed).

the inaccuracies in the PSF, the observed superiority of the RCTLS filter was expected. However, in the comparison with the regularized modified LMMSE filter, the RCTLS filter overcame the "handicap" of not having any information about the source image. This demonstrated beyond any doubt the advantages of the proposed approach for restoration problems where the knowledge of the PSF is erroneous.

In summing up this paper, two comments are in order. First, using the diagonalization properties of the DFT, it is relatively straightforward to derive a regularized TLS (RTLS) estimator based on the minimization of $\mathbf{u}^t\mathbf{W}\mathbf{u}$ in (14). However, in this case, as already mentioned earlier, this estimator does not have an ML interpretation and thus the desirable properties that stem from it. We verified this by deriving and experimentally comparing the RTLS estimator to the RCTLS one. In all our experiments we found that the RCTLS estimator yields higher ISNR's than the RTLS one. Second, the RCTLS estimator can be generalized to handle color noise models for the errors in both $\mathbf{H}$ and $\mathbf{g}$. If the covariance matrices of these errors are circulant the DFT domain expression of the RCTLS estimator will contain their eigenvalues instead of ${\sigma_h}^2$ and ${\sigma_g}^2$. This generalization can be very useful in cases that additional prior knowledge about the nature of the error in the PSF is available. For example, a PSF that is band- or space-limited and the bandwidth or the spatial support are known.

Appendix A

Let $\mathbf{W}$ be the $N \times N$ DFT matrix [11]. Inserting $\mathbf{W}^H\mathbf{W}$ into (28), where $\mathbf{W}^H$ is the Hermitian of $\mathbf{W}$, we obtain

$$P(\mathbf{f}) = (\bar{\mathbf{H}}\mathbf{f} - \mathbf{g})^H\mathbf{W}^H\mathbf{W}(\mathbf{L}\mathbf{L}^H)^{-1}\mathbf{W}^H\mathbf{W}(\bar{\mathbf{H}}\mathbf{f} - \mathbf{g}) + \lambda(\mathbf{Q}\mathbf{f})^H\mathbf{W}^H\mathbf{W}(\mathbf{Q}\mathbf{f}). \quad (58)$$

Now, examining the elements in (58) separately, and using the diagonalization properties of the DFT for circulant matrices, we obtain

$$\mathbf{W}(\bar{\mathbf{H}}\mathbf{f} - \mathbf{g}) = \mathbf{W}\bar{\mathbf{H}}\mathbf{W}^H\mathbf{W}\mathbf{f} - \mathbf{W}\mathbf{g} = \mathbf{D}_{\bar{H}}\mathbf{F} - \mathbf{G} \quad (59)$$

$$(\bar{\mathbf{H}}\mathbf{f} - \mathbf{g})^H\mathbf{W}^H = [\mathbf{W}(\bar{\mathbf{H}}\mathbf{f} - \mathbf{g})]^H = (\mathbf{D}_{\bar{H}}\mathbf{F} - \mathbf{G})^H \quad (60)$$

$$\mathbf{W}\mathbf{Q}\mathbf{f} = \mathbf{W}\mathbf{Q}\mathbf{W}^H\mathbf{W}\mathbf{f} = \mathbf{D}_Q\mathbf{F} \quad (61)$$

$$(\mathbf{Q}\mathbf{f})^H\mathbf{W}^H = (\mathbf{W}\mathbf{Q}\mathbf{f})^H = (\mathbf{D}_Q\mathbf{F})^H \quad (62)$$

$$\mathbf{W}(\mathbf{L}\mathbf{L}^H)^{-1}\mathbf{W}^H = [\mathbf{W}(\mathbf{L}\mathbf{L}^H)\mathbf{W}^H]^{-1} = (\mathbf{D}_L)^{-1} \quad (63)$$

where $\mathbf{D}_{\bar{H}}$ and $\mathbf{D}_Q$ are

$$\mathbf{D}_{\bar{H}} = \text{diag}\,[\bar{H}(0), \bar{H}(1), \cdots, \bar{H}(N-1)] \quad (64)$$

$$\mathbf{D}_Q = \text{diag}\,[Q(0), Q(1), \cdots, Q(N-1)] \quad (65)$$

and

$$\mathbf{D}_L = \text{diag}\,[{\sigma_h}^2|F(0)|^2 + {\sigma_g}^2, \cdots, {\sigma_h}^2|F(N-1)|^2 + {\sigma_g}^2]. \quad (66)$$

Having established the above, (58) can be transformed into

$$P(\mathbf{F}) = \sum_{i=0}^{N-1}\left\{\frac{|\bar{H}(i)F(i) - G(i)|^2}{{\sigma_h}^2|F(i)|^2 + {\sigma_g}^2} + \lambda|Q(i)|^2|F(i)|^2\right\}. \quad (67)$$

Since each term in (67) is nonnegative, minimizing it is equivalent to minimizing each component of the sum, with respect to each frequency, separately. Therefore, the RCTLS solution in the DFT domain can be obtained via

$$\min_{F(i)}\{P(F(i))\}, \text{ for } i = 0, 1, \cdots, N-1 \quad (68)$$

where the $P(F(i))$ are given by

$$P(F(i)) = \frac{|\bar{H}(i)F(i) - G(i)|^2}{{\sigma_h}^2|F(i)|^2 + {\sigma_g}^2} + \lambda|Q(i)|^2|F(i)|^2. \quad (69)$$

Appendix B

According to (42), the bias in the spatial domain is equal to

$$\mathbf{b} = E\{\Delta\mathbf{f}\} = -\lambda(\mathbf{A}\bar{\mathbf{H}} + \lambda\mathbf{Q}^t\mathbf{Q})^{-1}\mathbf{Q}^t\mathbf{Q}\mathbf{f}_0. \quad (70)$$

Taking the DFT of b, we have

$$\mathbf{W}\mathbf{b} = -\lambda[\mathbf{W}\mathbf{A}\mathbf{W}^H\mathbf{W}\bar{\mathbf{H}}\mathbf{W}^H + \lambda\mathbf{W}\mathbf{Q}^H\mathbf{W}^H\mathbf{W}\mathbf{Q}\mathbf{W}^H]^{-1}\mathbf{W}\mathbf{Q}^H\mathbf{W}^H\mathbf{W}\mathbf{Q}\mathbf{W}^H\mathbf{W}\mathbf{f}_0 \quad (71)$$

where

$$\mathbf{W}\mathbf{A}\mathbf{W}^H = \mathbf{W}\bar{\mathbf{H}}\mathbf{W}^H\mathbf{W}(\mathbf{L}_0\mathbf{L}_0{}^H)^{-1}\mathbf{W}^H. \quad (72)$$

Using (59) through (66), we obtain in the DFT domain

$$\mathbf{B} = -\sum_{i=0}^{N-1}\frac{\lambda|Q(i)|^2|F_0(i)|}{\frac{|\bar{H}(i)|^2}{{\sigma_h}^2|F_0(i)|^2 + {\sigma_g}^2} + \lambda|Q(i)|^2} \quad (73)$$

where $\mathbf{B}$ is the DFT of vector b. Similarly, one gets

$$\mathbf{b}^H\mathbf{W}^H = (\mathbf{W}\mathbf{b})^H \quad (74)$$

and

$$tr[\mathbf{b}\mathbf{b}^H] = \sum_{i=0}^{N-1}\frac{\lambda^2|Q(i)|^4|F_0(i)|^2}{\left[\frac{|\bar{H}(i)|^2}{{\sigma_h}^2|F_0(i)|^2 + {\sigma_g}^2} + \lambda|Q(i)|^2\right]^2}. \quad (75)$$

Taking the derivative of (75) with respect to λ, we have

$$\frac{\partial tr[\mathbf{b}\mathbf{b}^H]}{\partial\lambda} = \sum_{i=0}^{N-1}\frac{2\lambda|Q(i)|^4|F_0(i)|^2\frac{|\bar{H}(i)|^2}{{\sigma_h}^2|F_0(i)|^2 + {\sigma_g}^2}}{\left[\frac{|\bar{H}(i)|^2}{{\sigma_h}^2|F_0(i)|^2 + {\sigma_g}^2} + \lambda|Q(i)|^2\right]^3}. \quad (76)$$

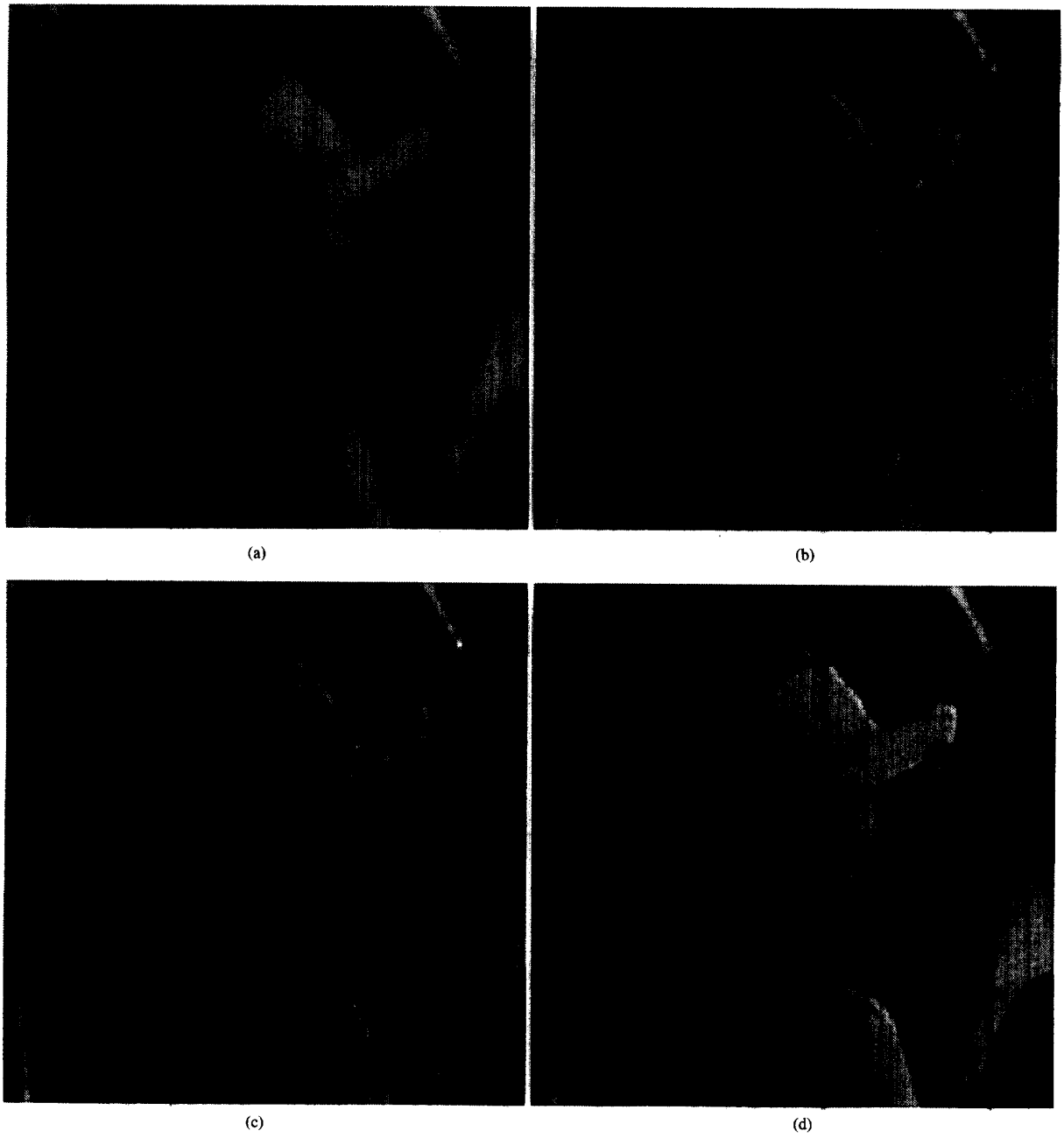

(a) (b) (c) (d)

Fig. 5. Experiment 3. (a) Degraded image; (b) LMMSE estimate; (c) RLS estimate; (d) RCTLS estimate.

Clearly, $tr[\mathbf{b}\mathbf{b}^H]$ is a strictly positive, monotonically increasing function of λ, for $\lambda > 0$.

Following similar steps as above the following can be obtained for the variance in the DFT domain. From (43), we directly obtain

$$\mathbf{C} = E\{(\mathbf{A}\bar{\mathbf{H}} + \lambda\mathbf{Q}^t\mathbf{Q})^{-1}[\mathbf{A}\mathbf{L}_0\mathbf{u}\mathbf{u}^t\mathbf{L}_0^t\mathbf{A}^t] (\mathbf{A}\bar{\mathbf{H}} + \lambda\mathbf{Q}^t\mathbf{Q})^{-t}\}. \tag{77}$$

Furthermore

$$\mathbf{C} = (\mathbf{A}\bar{\mathbf{H}} + \lambda\mathbf{Q}^t\mathbf{Q})^{-1}[\mathbf{A}\mathbf{L}_0\mathbf{R}_u\mathbf{L}_0{}^t\mathbf{A}^t](\mathbf{A}\bar{\mathbf{H}} + \lambda\mathbf{Q}^t\mathbf{Q})^{-t} \tag{78}$$

where $\mathbf{R}_u$ is the covariance matrix given by

$$\mathbf{R}_u = E\{\mathbf{u}\mathbf{u}^t\}. \tag{79}$$

From the definition of $\mathbf{u}$ in (9) and the assumed properties of the noise $\Delta\mathbf{H}$ and $\Delta\mathbf{g}$, it is clear that $\mathbf{R}_u = \mathbf{I}$, where $\mathbf{I}$ is the $2N \times 2N$ identity matrix. Finally, in the DFT domain the

$$\frac{\partial^2 \varepsilon}{\partial \lambda^2} = \sum_{i=0}^{N-1} \frac{\frac{2|Q(i)|^4|\bar{H}(i)|^2}{\sigma_h{}^2|F_0(i)|^2+\sigma_g{}^2}}{\left[\frac{|\bar{H}(i)|^2}{\sigma_h{}^2|F_0(i)|^2+\sigma_g{}^2} + \lambda|Q(i)|^2\right]^4} \times \frac{\left\{|F_0(i)|^2\left(\frac{|\bar{H}(i)|^2}{\sigma_h{}^2|F_0(i)|^2+\sigma_g{}^2} + \lambda|Q(i)|^2\right) - 3\lambda|Q(i)|^2|F_0(i)|^2 + 3\right\}}{\left[\frac{|\bar{H}(i)|^2}{\sigma_h{}^2|F_0(i)|^2+\sigma_g{}^2} + \lambda|Q(i)|^2\right]^4} \tag{85}$$

variance can be written as

$$tr[\mathbf{C}] = \sum_{i=0}^{N-1} \frac{\frac{|\bar{H}(i)|^2}{\sigma_h{}^2|F_0(i)|^2+\sigma_g{}^2}}{\left[\frac{|\bar{H}(i)|^2}{\sigma_h{}^2|F_0(i)|^2+\sigma_g{}^2} + \lambda|Q(i)|^2\right]^2}. \tag{80}$$

Taking the derivative of (80) with respect to λ, we have

$$\frac{\partial tr[\mathbf{C}]}{\partial \lambda} = -\sum_{i=0}^{N-1} \frac{2\frac{|\bar{H}(i)|^2}{\sigma_h{}^2|F_0(i)|^2+\sigma_g{}^2}|Q(i)|^2}{\left[\frac{|\bar{H}(i)|^2}{\sigma_h{}^2|F_0(i)|^2+\sigma_g{}^2} + \lambda|Q(i)|^2\right]^3}. \tag{81}$$

Clearly, $tr[\mathbf{C}]$ is a strictly positive, monotonically decreasing function of λ, for $\lambda > 0$.

Taking the derivative of the MSE ε, with respect to λ, yields

$$\frac{\partial \varepsilon}{\partial \lambda} = \sum_{i=0}^{N-1} \frac{2\left(\lambda|Q(i)|^4|F_0(i)|^2 - |Q(i)|^2\right)\frac{|\bar{H}(i)|^2}{\sigma_h{}^2|F_0(i)|^2+\sigma_g{}^2}}{\left[\frac{|\bar{H}(i)|^2}{\sigma_h{}^2|F_0(i)|^2+\sigma_g{}^2} + \lambda|Q(i)|^2\right]^3}. \tag{82}$$

From (82) it is straightforward to see that

$$\frac{\partial \varepsilon}{\partial \lambda} < 0 \text{ for } 0 \le \lambda < \left[\frac{1}{|Q(i)|^2|F_0(i)|^2}\right]_{min} \tag{83}$$

and

$$\frac{\partial \varepsilon}{\partial \lambda} > 0 \text{ for } \left[\frac{1}{|Q(i)|^2|F_0(i)|^2}\right]_{max} \le \lambda < \infty. \tag{84}$$

By examining the second derivative of the MSE ε with respect to λ, it is straightforward to get the equation as shown in (85) at the top of the page. Clearly, from (85), if for any $i = 0, \cdots, N-1$, λ satisfies

$$\begin{aligned} &|F_0(i)|^2\left(\frac{|\bar{H}(i)|^2}{\sigma_h{}^2|F_0(i)|^2+\sigma_g{}^2} + \lambda|Q(i)|^2\right) \\ &-3\lambda|Q(i)|^2|F_0(i)|^2 + 3 \ge 0 \end{aligned} \tag{86}$$

the candidate for the extremum ($\frac{\partial \varepsilon}{\partial \lambda} = 0$) becomes a minimum. Inequality in (86) is equivalent to

$$\lambda \le \left[\frac{1}{2|Q(i)|^2}\frac{|\bar{H}(i)|^2}{\sigma_h{}^2|F_0(i)|^2+\sigma_g{}^2} + \frac{3}{2}\frac{1}{|Q(i)|^2|F_0(i)|^2}\right]_{min}. \tag{87}$$

Using (83), (84), and (87), we conclude that ε has a minimum value in the interval

$$\begin{aligned} &[(\frac{1}{|Q(i)|^2|F_0(i)|^2})_{min}, (\frac{1}{2|Q(i)|^2}\frac{|\bar{H}(i)|^2}{\sigma_h{}^2|F_0(i)|^2+\sigma_g{}^2} \\ &+ \frac{3}{2}\frac{1}{|Q(i)|^2|F_0(i)|^2})_{min}]. \end{aligned} \tag{88}$$

Therefore, a value of the parameter λ can be found such that the total MSE of the RCTLS estimate is smaller than the MSE of the CTLS estimate.

ACKNOWLEDGMENT

The authors acknowledge two anonymous reviewers for their insightful comments and suggestions that helped improve the quality of this paper.

REFERENCES

[1] T. J. Abatzoglou, J. M. Mendel, and G. A. Harada, "The constrained total least-squares technique and its applications to harmonic superresolution," *IEEE Trans. Signal Processing*, vol. 39, no. 5, pp. 1070–1087, May 1991.

[2] H. Andrews and B. Hunt, *Digital Image Restoration*. Englewood Cliffs, NJ: Prentice-Hall, 1977.

[3] P. L. Combettes and H. J. Trussell, "Methods for digital restoration of signals degraded by a stochastic impulse response," *IEEE Trans. Acoust., Speech, Signal Processing*, vol. 37, no. 3, pp. 393–401, Mar. 1989.

[4] G. Demoment, "Image reconstruction and restoration: Overview of common estimation problems," *IEEE Trans. Acoust., Speech, Signal Processing*, vol. 37, pp. 2024–2036, Dec. 1989.

[5] X. Fan, "The constrained total least squares with regularization and its use in ill-conditioned signal restoration," Ph.D. thesis, Elec. Comput. Eng. Dept., Mississippi State Univ., Dec. 1992.

[6] N. P. Galatsanos and A. K. Katsaggelos, "Methods for choosing the regularization parameter and estimating the noise variance in image restoration and their relation," *IEEE Trans. Image Processing*, vol. 1, no. 3, pp. 322–336, July 1992.

[7] G. H. Golub and C. F. Van Loan, "An analysis of total least-squares problem," *SIAM J. Numer. Anal.*, vol. 17, pp. 883–893, 1980.

[8] ——, *Matrix Computations*. Baltimore, MD: Johns Hopkins Univ. Press, 1989.

[9] L. Guan and R. K. Ward, "Deblurring random time-varying blur," *J. Opt. Soc. Amer. A.*, vol. 6, no. 11, pp. 1727–1737, Nov. 1989.

[10] S. V. Huffel and J. Vandewalle, *The Total Least-Squares Problem*. New York: SIAM, 1991.

[11] B. R. Hunt, "The application of constrained least-squares estimation to image restoration by digital computer," *IEEE Trans. Comput.*, vol. C-22, no. 9, pp. 805–812, Sept. 1973.

[12] K. T. Lay and A. K. Katsaggelos, "Image identification and restoration based on the expectation-maximization algorithm," *Opt. Eng.*, vol. 29, pp. 436–445, May 1990.

[13] R. L. Lagendijk, J. Biemond, and D. E. Boekee, "Identification and restoration of noisy blurred images using the expectation-maximization algorithm," *IEEE Trans. Acoust., Speech, Signal Processing*, vol. 38, pp. 1180–1191, July 1990.

[14] J. M. Mendel, *Lessons in Digital Estimation Theory*. Englewood Cliffs, NJ: Prentice-Hall, 1987.

[15] V. Z. Mesarović, "Image restoration using regularized constrained total least-squares," Master's thesis, ECE Dept., Ill. Inst. of Technol., Chicago, Dec. 1993.

[16] B. P. Flannery, W. H. Press, S. A. Teukolsky, and W. T. Vetterling, *Numerical Recipes in C*. Cambridge, MA: Cambridge Univ. Press, 1988.

[17] S. J. Reeves and R. M. Mersereau, "Optimal estimation of the regularization parameter and stabilizing functional for regularized image restoration," *Opt. Eng.*, vol. 29, pp. 446–454, May 1990.

[18] ——, "Blur identification by the method of generalized cross-validation," *IEEE Trans. Image Processing*, vol. 1, no. 3, pp. 301–311, July 1992.

[19] A. E. Savakis and H. J. Trussell, "On the accuracy of PSF representation in image restoration," *IEEE Trans. Image Processing*, vol. 2, no. 2, pp. 252–259, Apr. 1993.

[20] A. Tikhonov and V. Arsenin, *Solution of Ill-Posed Problems*. New York: Wiley, 1977.

[21] R. K. Ward and B. E. A. Saleh, "Restoration of images distorted by systems of random impulse response," *J. Opt. Soc. Amer. A.*, vol. 2, no. 8, pp. 1254–1259, Aug. 1985.

[22] ——, "Deblurring random blur," *IEEE Trans. Acoust., Speech, Signal Processing*, vol. 35, no. 10, pp. 1494–1498, Oct. 1987.
[23] Y. Yang, N. P. Galatsanos, and H. Stark, "Projection-based blind deconvolution," *J. Opt. Soc. Amer. A.*, vol. 11, no. 9, Sept. 1994.
[24] D. C. Youla, "Generalized image restoration by the method of alternating orthogonal projections," *IEEE Trans. Circuits Syst. [Video Technol.]*, vol. 25, no. 9, pp. 694–702, Sept. 1978.

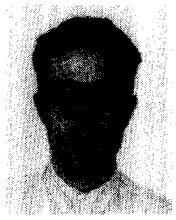

Vladimir Z. Mesarović was born in Belgrade, Yugoslavia, in 1967. He received the Diploma degree in electrical engineering from the University of Belgrade, Belgrade, Yugoslavia, in 1992 and the M.S.E.E. degree from the Illinois Institute of Technology, Chicago, in 1993. Currently, he is a Ph.D. candidate at the Department of Electrical and Computer Engineering at Illinois Institute of Technology, Chicago, IL.

His current research interests are in signal and image recovery.

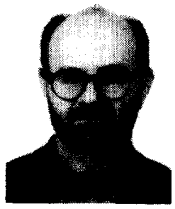

Nikolas P. Galatsanos (S'84–M'85) was born in Athens, Greece, in 1958. He received the Diploma degree in electrical engineering from the National Technical University of Athens, Athens, Greece, in 1982. He received the M.S. and the Ph.D. degrees, both in electrical and computer engineering from the University of Wisconsin-Madison in 1984 and 1989, respectively.

Since August of 1989, he has been on the faculty of the Department of Electrical and Computer Engineering at the Illinois Institute of Technology, Chicago, where he is currently an Assistant Professor. His current research interests include image processing and multidimensional signal processing and, more specifically, recovery and compression of single and multichannel/frame images.

Dr. Galatsanos served as an associate editor for the IEEE TRANSACTIONS ON IMAGE PROCESSING.

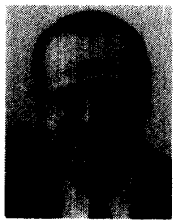

Aggelos K. Katsaggelos (S'80–M'85–SM'92) received the Diploma degree in electrical and mechanical engineering from the Aristotelian University of Thessaloniki, Thessaloniki, Greece, in 1979, and the M.S. and Ph.D. degrees, both in electrical engineering, from the Georgia Institute of Technology, Atlanta, in 1981 and 1985, respectively.

In 1985, he joined the Department of Electrical Engineering and Computer Science at Northwestern University, Evanston, IL, where he is currently an associate professor. During the 1986–1987 academic year, he was an assistant professor at Polytechnic University, Department of Electrical Engineering and Computer Science, Brooklyn, NY. His current research interests include image recovery, processing of moving images (motion estimation, enhancement, very low bit rate compression), and computational vision.

Dr. Katsaggelos is an Ameritech Fellow and a member of the Associate Staff, Department of Medicine, at Evanston Hospital. He is a member of SPIE, the Steering Committees of the IEEE TRANSACTIONS ON MEDICAL IMAGING and the IEEE TRANSACTIONS ON IMAGE PROCESSING, the IEEE Technical Committees on Visual Signal Processing and Communications and on Image and Multidimensional Signal Processing, the Technical Chamber of Commerce of Greece, and Sigma Xi. He has served as an associate editor for the IEEE TRANSCATIONS ON SIGNAL PROCESSING (1990-1992) and is currently an area editor for the journal *Graphical Models and Image Processing*. He is the editor of *Digital Image Restoration* (Springer-Verlag, Heidelberg, 1991) and the General Chairman of the 1994 Visual Communications and Image Processing Conference (Chicago, IL).